

## The study of erosive wear of the shaped elements of compressor station manifold of a gas pipeline

*Ya. V. Doroshenko\**, *T. I. Marko*, *Yu. I. Doroshenko*

*Ivano-Frankivsk National Technical University of Oil and Gas;  
15, Karpatska str., Ivano-Frankivsk, 76019, Ukraine*

Received: 30.09.2016 Accepted: 12.12.2016

### Abstract

The research is made to identify the places of intense strikes of liquid and solid particles to the wall of compressor station manifold of a gas pipeline, their erosive wear and to calculate the erosion rate.

There is carried out 3D modeling of compressor station piping and its shaped elements, where a complex movement of multiphase flows, change of their direction, swirl, strikes of discrete phases to the wall of a pipeline as well as erosive wear of the pipeline wall occur.

Based on the Lagrangian approach (the Discrete Phase Model) there were developed methods for modeling the erosive wear of compressor station manifold shaped elements (bends, T-junctions) using ANSYS Fluent R17.0 Academic software. A mathematical model is based on solving the Navier–Stokes, continuity, discrete phases motion and the Finney equations, two–parameter  $k-\varepsilon$  Launder–Sharma turbulence model with appropriate initial and boundary conditions. The simulation was performed for different motion patterns of gas (gas moves through T-junction run-pipe to the T-junction branch; gas moves through the branch of T-junction to the T-junction run-pipe, in which a portion of gas stream flows in one side of the run-pipe, and the rest of the gas stream – in the other one; gas moves through the T-junction branch to one side of the T-junction run-pipe).

The simulation results were visualized in ANSYS Fluent R17.0 Academic postprocessor by building concentration fields of a discrete phase and erosion rate fields at shaped elements contours. Having studied the obtained results there were identified places of intense strikes of liquid and solid particles to the wall of shaped elements of compressor station manifold, the intensive erosive wear of a pipeline wall and there was calculated the erosion rate.

Keywords: *a bend, a discrete phase, concentration fields, Finney equation, T-junction, the Lagrangian approach.*

Compressor station manifold of trunk gas pipelines consists of straight pipeline sections, curves (branches) of hot bending, T-junctions, reducers, covering fitting. A complex turbulent motion of gas flow and the change in the direction of its movement, leading to strikes of liquid and solid particles (the discrete phase) in the flow of natural gas (a solid phase) to the wall of the pipeline and resulting in erosive wear of a pipe wall, occur in T-junctions and curves of hot bending. The erosive wear is a factor that reduces the residual life of pipelines. If compressor station manifold is not properly monitored, the erosive wear can lead to pipeline ruptures and loss of products, and these facts are life-threatening and can cause damage to buildings in the territory of compressor stations. The erosive wear of a pipe wall is especially dangerous for pipelines with the service life exceeding 35–40 years. The gas transportation system of Ukraine primarily consists of such pipelines. Therefore, a comprehensive study of the erosive wear of gas pipelines wall is particularly relevant.

To assess the efficiency of erosively worn compressor station manifold and calculate their remaining resource it is necessary to know the erosion rate, places of manifold erosive wear and a geometric shape of the defective inner surface. Such information also enables to improve designs of the manifold for their long service life.

It is very difficult to accurately predict the erosive wear of compressor station manifold because of the wide range of parameters that affect their placement and size, including the flow rate of liquid and solid particles, concentration, diameter, particles density, the mode of flow, gas temperature, geometry of the shaped elements, material of wall, etc.

Today these problems can be solved in the shortest time by means of the software package ANSYS Fluent, which enables to simulate the erosive wear of gas pipelines shaped elements and calculate the value of erosive wear.

### An analysis of recent domestic and foreign studies

The erosive wear of shaped elements occurs in various pipelines (gas pipelines, oil pipelines, nitrogen pipelines, steam pipelines of nuclear and thermal power stations, pneumatic transport, etc.). This causes interest of many researchers to study the processes of the erosive wear of pipe walls.

\* Corresponding author:  
ya.doroshenko@nung.edu.ua

© 2016, Ivano-Frankivsk National Technical University of Oil and Gas.  
All rights reserved.

Many modern scientists are involved in computer modeling of the erosive wear of pipeline shaped elements. Their studies confirm that these software systems are effective means for identifying places and calculating the erosion rate of pipeline shaped elements.

In particular V. Abdolkarimi and R. Mohammadikhah [1] studied the erosive wear of the gas pipeline bend with the outside diameter of 1420 mm and the angle of 90° under the pressure of 8 MPa by means of the computer modeling in ANSYS Fluent 6.3. Mass flow of gas at the inlet was 3780 kg/s. The maximum erosive wear was found between 40° and 65° angles of the bend, the calculated maximum rate of erosive wear was  $3.2 \cdot 10^{-9}$  m/s. Having compared the results of numerical calculations with the results of experimental measurements, the authors concluded that CFD (computational fluid dynamics) modeling is a powerful tool for assessing the erosive wear of various industrial facilities.

In his master's thesis A. Abdua (Blekinge Institute of Technology Karlskrona, Sweden) [2] investigated the effect of the impact velocity of the sand and condensation drops upon the erosive wear of gas pipelines bends of the inner diameter of 50.8 mm and the rotation angle of 90° by means of computer simulation. There were set three different velocities of liquid and solid particles – 12, 19 and 28 m/s. According to the simulation results there was determined that particles velocity was proportional to the rate of erosive wear and significantly affected the average and maximum rates of the erosive wear. It was also observed that the density of the liquid droplets affected the location of the maximum erosive wear. Thus the maximum erosive wear was found almost in the middle of the bend when the density of liquid droplets was low. If the density of liquid droplets increases, the location of the maximum erosive wear shifts toward the flow outlet of the bend and the beginning of the adjacent pipe.

M. Azimian and H. Bart [3] studied the rate of erosive wear of the bend and T-junction with a diameter of 25 mm by means of computer simulation. The operating environment was liquid with solid particles. Places of the shaped elements erosive wear, the maximum rate of erosive wear were found. It was also found that if the liquid with solid particles is transported by the pipeline, the erosive wear of the T-junction is greater than that of the bend.

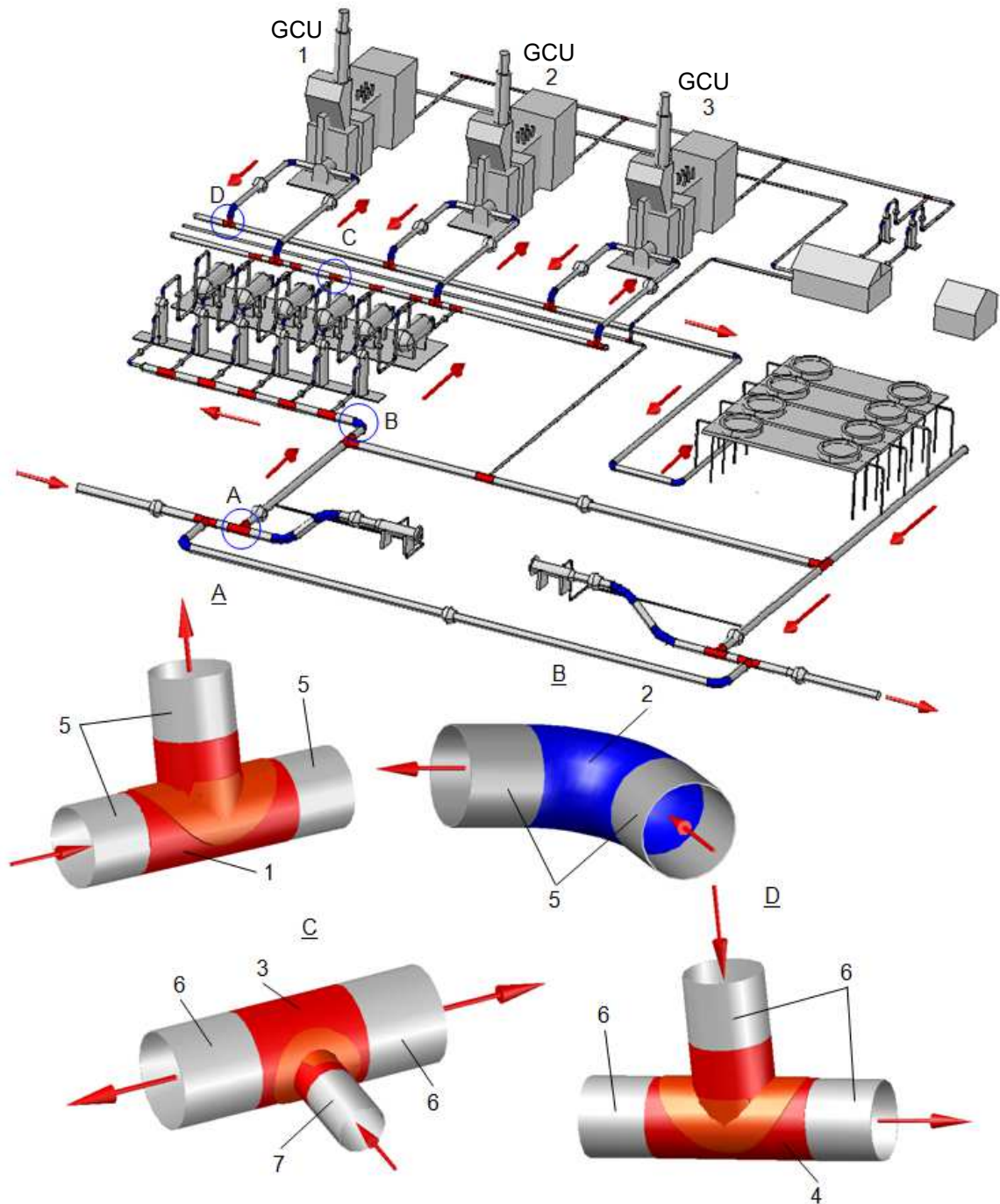
Q. Mazumder [4] and H. Zhang, Y. Tan and D. Yang [5] studied the dependence of the value and location of the erosive wear of the T-junction and the U-bend pipe upon the velocity of transported air and water, the velocity and size of sand particles by means of computer simulation. It is found that the maximum erosive wear is about 40° below the place of direct strikes of particles in the T-junction and the U-bend pipe, and the place of the maximum erosive wear of the T-junction depends on the discrete phase velocity. If the discrete phase velocity increases, the place of the maximum erosive wear of the T-junction moves down the flow. If the air is transported by the pipeline, then with increasing the size of sand particles, the place of

the maximum erosive wear of the U-bend approaches the flow inlet in the U-bend, and if the water is transported by the pipeline, then with increasing the size of sand particles, the place of the maximum erosive wear of the U-bend moves away from the flow inlet in the U-bend. The same effects were observed for different velocities of operating media. It was also discovered that air and water velocities do not have a significant impact on the location of the erosive wear of the U-bend.

Z. Hongjun and L. Yuanhua [6] investigated the effects of pipeline geometrical parameters, flow parameters and characteristics of a discrete phase (sand) on the value of the erosive wear of nitrogen pipelines bends by means of computer simulation and the software package ANSYS Fluent. It is found out that the smaller the diameter of the pipeline and the smaller the bending angle of the T-junction, the larger the flow rate; the greater the volume fraction of sand and the bigger diameter of the sand grain, the greater is the value of erosive wear of nitrogen pipelines bends. I. Dorina [7] carried out similar studies in pneumatic transport of anthracite powder, which is extremely abrasive. It is studied by means of computer simulation that the value of the erosive wear of pneumatic actuator bend depends on the ratio between the radius of its bending, the pipe diameter and the air flow rate of anthracite powder. It is found out that the most significant factor that affects the value of erosion rate of the bend is the velocity of anthracite powder particles in the air flow. By means of computer simulation H. Hadžiahmetović [8] and M. Tarek [9] compared the results of the erosive wear of pneumatic actuator bends of round and square sections with experimental data and made sure of their convergence in the places of the maximum erosive wear. It was determined that a flow rate and particle size have the greatest effect on the erosive wear. Very small particles (with the diameter less than 10 μm) move with the main flow and virtually do not hit the wall of the pipeline because they are light. Usually they hit at small angles of attack and it does not lead to a significant erosive wear. Larger particles tend to hit the wall. Thus, the greater the flow rate and the larger particles, the greater the erosive wear.

Information on the erosive wear of the shaped elements of compressor station manifold is received on the basis of the external inspection by ultrasonic flaw detectors, requiring special permits, financial and time costs, excavation of underground sites of pipelines. Erosive wear test of compressor station manifold shaped elements are not provided by any Ukrainian regulations and experts, who carry out these inspections, define them based on their logical reasoning and their acquired experience. These facts do not always allow revealing the places of the maximum erosion that is no less important than the precise determination of the erosive wear.

The objective of the study is to develop scientific and methodological foundations of complex numerical modeling of erosive wear of compressor station manifold, identify places of erosive wear of shaped elements and calculate the extent of erosive wear.



1 – the internal flush-jointed T-junction with reinforcing patches 1420×28 – 1420×28 (OST 102–61 [10]); 2 – bend 90°1420×24 (Gas Specifications 102-488/1 [11]); 3 – welded T-junction with reinforcing patches 1020×18 – 529×10 (OST 102–61 [10]); 5 – the pipe 1420×18.7; 6 – the pipe 1020×12.3; 7 – the pipe 529×7

**Figure 1 – Compressor station layout**

The largest number of pipeline shaped elements (bends, T-junctions, reducers) is contained in compressor stations manifold (Fig. 1), underground gas storages, and gas distribution stations.

The change in direction of product flow to 90° (except for the bends at the inlet and outlet of the in-tube compartments) occurs in bends of compressor station manifold (Fig. 1). There are different schemes of gas movement in the T-junctions of compressor station manifold:

gas moves through the T-junction 1 run-pipe (Fig. 1) to the T-junction branch;

gas moves through the T-junction 3 branch (Fig. 1) to the T-junction run-pipe, where part of gas stream flows in one direction of the line, and the rest of gas – in the opposite direction;

gas moves through the T-junction 4 branch (Fig. 1) in either direction of the line.

We know that natural gas transported by pipelines contains liquid and solid particles (contaminations). Gas

condensate, water, oil and other hydrocarbons belong to the liquid discrete phase. The rock, sand, slag, exfoliated from the inner wall of the pipe and carried from well deposits, the products of in-tube corrosion belong to the solid discrete phase.

There are different reasons for the presence of contaminants in the inner cavity of pipelines. Firstly, it is the poor quality of gas purification in the fishery and compressor stations, liquids condensing from the gas stream at favorable thermodynamic conditions while gas pumping in the pipeline, passing of bearing lubrication in gas pumping units, poor cleaning of the inner cavity of the pipeline before its exploitation. The chemical reaction between the pipe metal and liquid pollution, accumulated in the lowered fields of pipelines, lead to corrosion and formation of solid particles.

When moving by the shaped elements of compressor station manifold, liquid and solid particles hit the wall of the pipeline, leading to erosive wear of the pipeline. For timely and quality inspection of shaped elements of compressor stations manifold, and the improvement of existing structures we should know the places of their maximum erosive wear and forecast the value of their erosive wear.

The erosive wear of shaped elements of compressor station manifold can be studied at the most by computer simulation of three-dimensional turbulent flows by means of the ANSYS Fluent R17.0 Academic software. Mathematical models and numerical algorithms of this complex meet international standards.

To simulate the erosive wear in ANSYS Fluent there is laid the Lagrangian Discrete Phase Model (DPM). The basis of the Lagrangian approach is the consideration of the motion of individual particles (or groups of particles) of the discrete phase. The Lagrangian DPM enables us to explore the trajectory of discrete phase particles in the solid phase by solving the differential equation of particle motion. The discrete phase can be solid, as bubbles in the liquid or as gas drops. The model allows for the two-way exchange of mass, momentum and energy of particles with the solid phase. The DPM model is used for small values of particles volume concentration because the interaction of particles with each other is indirectly taken into account. The advantage of the DPM model is that it allows us to accurately take into account the nature of the interaction of the discrete phase with the wall. In the model of interaction between the discrete phase and the wall there is the additional model of the wall erosion. In addition, it is much easier to take into account the secondary decay of the discrete phase (in case of drops or bubbles) within the DPM model. The disadvantage of the DPM model is the limit of the local volume concentration of particles (less than 10 %).

An integrated numerical simulation has three stages:

- simulation of the gas flow (solid phase) in the shaped elements of pipelines;
- simulation of liquid and solid particles motion with shaped elements of pipelines in the gas stream;
- calculation of the erosive wear of pipelines shaped elements.

The motion of a solid phase in ANSYS Fluent is simulated by numerical solution of equations describing the general motion of the gaseous medium. These are the Navier-Stokes equation (1), which expresses the law of momentum conservation (or Reynolds (2) if the flow is turbulent) and the continuity equation (3), which expresses the law of mass conservation

$$\frac{\partial}{\partial t}(\rho u_i) + \frac{\partial}{\partial x_j}(\rho u_i u_j) = -\frac{\partial p}{\partial x_i} + \frac{\partial}{\partial x_j} \left( \mu \left( \frac{\partial u_i}{\partial x_j} + \frac{\partial u_j}{\partial x_i} \right) \right) + f_i, \quad (1)$$

$$\frac{\partial}{\partial t}(\rho u_i) + \frac{\partial}{\partial x_j}(\rho u_i u_j) + \frac{\partial}{\partial x_j}(\rho u_i' u_j') = -\frac{\partial p}{\partial x_i} + \frac{\partial}{\partial x_j} \left( \mu \left( \frac{\partial u_i}{\partial x_j} + \frac{\partial u_j}{\partial x_i} \right) \right) + f_i, \quad (2)$$

$$\frac{\partial \rho}{\partial t} + \frac{\partial}{\partial x_j}(\rho u_j) = 0, \quad (3)$$

where  $x_i, x_j$  are the coordinates;  $t$  is time;  $u_i, u_j$  are velocity components;  $\rho$  is the density of gas;  $\mu$  is molecular dynamic viscosity of the gas;  $f_i$  is a term that takes into account the effect of mass forces;  $p$  is the pressure;  $u_i$  are time-averaged values of velocity;  $u_i'$  are the components of velocity pulsation [12].

Boundary conditions usually include the distribution of all components of velocity in the inlet section and the vanishing of the first derivatives (in the direction of flow) of velocity components in the outlet section. Pressure is only the first derivative in the equations, so you only need to indicate the pressure at any one point of the computational geometry.

These equations are closed by two-parameter  $k - \varepsilon$  (where  $k$  is the turbulence energy,  $\varepsilon$  is the rate of dissipation of the turbulence energy) turbulence model, which involves solving the following equations in ANSYS Fluent:

$$\text{transport of the turbulence energy } k \\ \frac{\partial(\rho k)}{\partial t} + \nabla(\rho \mathbf{u}k) = \nabla \left( \left( \mu + \frac{\mu_t}{\sigma_k} \right) \nabla k \right) + \mu_t G - \rho \varepsilon; \quad (4)$$

transport equation for dissipation rate of the turbulence kinetic energy  $\varepsilon$

$$\frac{\partial(\rho \varepsilon)}{\partial t} + \nabla(\rho \mathbf{u}\varepsilon) = \nabla \left( \left( \mu + \frac{\mu_t}{\sigma_\varepsilon} \right) \nabla \varepsilon \right) + C_1 \frac{\varepsilon}{k} \mu_t G - C_2 \rho \frac{\varepsilon^2}{k}; \quad (5)$$

where  $\mathbf{u}$  is the flow rate of gas;  $\mu_t$  is the turbulent dynamic viscosity of gas;  $G$  is the mass flow;  $\sigma_k, \sigma_\varepsilon, C_1, C_2$  are experimentally obtained numeric constants ( $\sigma_k = 1, \sigma_\varepsilon = 1.3, C_1 = 1.44, C_2 = 1.92$ ).

The turbulence model  $k - \varepsilon$  is the so-called "high Reynolds" model created on the basis of averaging the Navier-Stokes equations and designed to calculate turbulent processes.

The substance, which is present in solid phase flow in the form of a discrete phase, does not form a continuum, and some particles interact with the continuous phase flow and with each other. For simulation of the discrete phase flow in a continuous phase there is applied the Lagrangian approach in ANSYS Fluent, i.e. the movement of individual particles is tracked under the influence of the forces of the solid phase flow.

It is believed that particles of the discrete phase are spheres. The forces influencing the particle are caused by the difference of the particle velocity and flow rate of the solid phase, and the displacement of the continuous phase medium with this particle. The equation of motion for this particle was derived in [13] and has the following form

$$m_p \frac{d\mathbf{u}_p}{dt} = 3\pi\mu d_p C_{cor} (\mathbf{u} - \mathbf{u}_p) + \frac{\pi d_p^3 \rho}{6} \frac{d\mathbf{u}}{dt} + \frac{\pi d_p^3 \rho}{12} \left( \frac{d\mathbf{u}}{dt} - \frac{d\mathbf{u}_p}{dt} \right) + \mathbf{F}_e - \frac{\pi d_p^3}{6} (\rho_p - \rho) \boldsymbol{\omega} \times (\boldsymbol{\omega} \times \mathbf{r}) - \frac{\pi d_p^3 \rho_p}{3} (\boldsymbol{\omega} \times \mathbf{u}_p), \quad (6)$$

where  $m_p$  is the particle mass,  $\mathbf{u}_p$  is the velocity of the particle;  $d_p$  is the diameter of the particle;  $\rho_p$  is the density of the particle;  $C_{cor}$  is the coefficient of viscous resistance;  $\mathbf{F}_e$  is the external force acting on the particle (such as gravity or strength of the electric field);  $\boldsymbol{\omega}$  is the angular velocity;  $\mathbf{r}$  is the radius of the vector (in case of considering the movement in the relative frame of reference).

The right side of the equation (6) is the sum of all forces acting on the particle, expressed in terms of mass and acceleration of the particle. The particle inhibition is the first term in the right side due to viscous friction to solid phase flow according to Stokes' law. The second term is the force applied to the particle, caused by the pressure drop, accelerated solid phase flow in the continuous phase, which surrounds the particle. The third term is the force required to accelerate the weight of the solid phase in the volume, which is repressed by the particle. These two terms should be considered when the density of the main phase is greater than the particles density. The fourth term ( $\mathbf{F}_e$ ) is the external force that influences directly upon the particle, such as the gravity or strength of the electric field. The last two terms are the centrifugal force and the Coriolis force, which take place only if the motion is considered in the relative frame of reference. In addition, some additional forces should be sometimes considered in the right side (6) (e.g. in case of significant temperature difference in the flow).

The equation (6) is a differential equation of the first order, in which the only unknown quantity is the particle velocity  $\mathbf{u}_p$ , and the argument is time  $t$ . The flow rate of the solid phase  $\mathbf{u}$  is considered as a known one and it is defined by solving the equations (1), (2),

(3) at all points of the medium. The initial data is the particle position at the initial time in addition to its size and properties. There is also indicated what should occur when particles hit the wall or another particle. The terms, which contain  $\mathbf{u}_p$ , are moved on the left side of equation (6) to perform the calculation. The velocity and position of the particle in each successive moment of time is determined by numerical integration of all the other terms of the equation (6) over time with some step  $\Delta t$ .

The algorithms, implemented in ANSYS Fluent, make it possible to simulate the impact of the discrete phase on the flow of the continuous phase. In the first approximation the density and viscosity of the continuous phase and some other values are multiplied by  $(1 - \alpha_p)$ , where  $\alpha_p$  is the specific volume occupied by the particles. In this case the changes in mass, momentum and energy of the particles are calculated at every step of the time, and these changes are added according to the equation of mass conservation (2), pulse (1) and the energy for the flow of the continuous phase. Thus, the calculation of the continuous phase flow and particle motion is performed jointly.

If the flow of the continuous phase is turbulent, the trajectory of particles is not deterministic, because it depends on the intensity and direction of turbulent fluctuations. Several boundary conditions, which correspond to different events that occur when the particles hit the wall, are implemented in modern software products: beating off as a result of elastic or inelastic hitting, sticking to the wall, sliding along the wall (depending on the physical properties and the angle of attack), passing through the wall (if the wall is porous), etc. Under certain conditions, there is also the possibility of splitting and merging simulation of water droplets or gas bubbles when they hit each other [14].

The calculation of the erosive wear is made using the Finney model, developed for rigid plastic materials by analyzing the equations of motion of a particle during its hitting the surface, by means of Ansys Fluent software. To estimate the amount of the surface material loss caused by the particle hitting there is investigated the trajectory of the particle motion. The following assumptions were made:

- cutting the surface is plastic deformation;
- cracks do not extend in front of the particle, which cuts the surface;
- material delamination is caused by the cutting action of particles.

This model can not be used for brittle materials.

According to the Finney model, the specific erosion rate (the surface mass removed from a surface unit per a unit of time) on the surface equals

$$E = K u_p^n f(\theta), \quad (7)$$

where  $K$  is the coefficient that depends on the elastic modulus of the wall material and the particle density;  $n$  is the exponent, which depends on the wall material (it varies from 2.3 to 2.5 for steel);  $f(\theta)$  is a dimensionless function that takes into account the

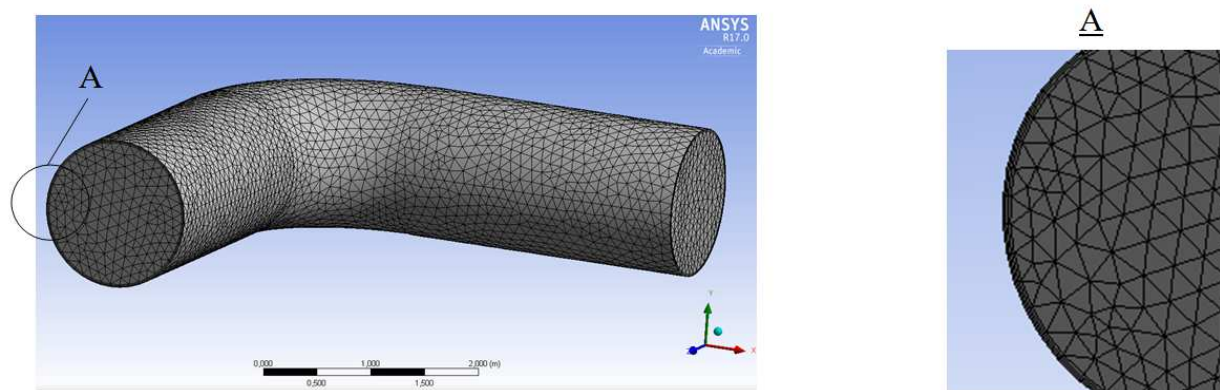


Figure 2 – The computed volumetric mesh

impact of the angle of attack  $\theta$  on the rate of the erosive wear. This function can be of different forms. For instance, it has the following form in [15]

$$f(\theta) = \begin{cases} A\theta^2 + B\theta, & \text{if } \theta \leq \varphi; \\ X\cos^2\theta \sin(W\theta) + Y\sin^2\theta + Z, & \text{if } \theta > \varphi, \end{cases} \quad (8)$$

where  $A, B, W, X, Y, Z, \varphi$  are empirical coefficients.

Three-dimensional models of the shaped elements of compressor station manifold, the design and geometric dimensions of which are identical to industrial designs (Fig. 1), are drawn in a Design Modeler geometric module of Ansys Fluent. Geometry of shaped elements meets the requirements of the standard OST 102–61 [10] and Gas Specifications 102-488/1 [11], which are widely spread in the gas industry. Moreover, shaped elements were drawn with surrounding pipes areas, geometric dimensions of which meet specifications. Pipe wall thickness was calculated based on the pressure in the place of shaped element location and in view of the fact that the pipelines of compressor station manifold belong to the highest category.

The estimated volumetric Automatic mesh was generated in Meshing–Fluent's preprocessing technology – the volume was filled with parallelepipeds, and if it was found impossible – triangular prisms were applied. The size of mesh elements was set as 0.09 m (Fig. 2). To better describe the near-boundary layer there was created the near-wall Inflation Layer with the lattice height of 0.09 m and the number of lattice layers 3 (Fig. 2). The calculation results were qualitatively visualized for this size of mesh elements.

When the program ANSYS Fluent was opened, double accuracy was set. A standard two-parameter model of turbulence  $k-\varepsilon$  was chosen in the program ANSYS Fluent, Models menu, Viscous tab. This model has three versions (Standard, RNG and Realizable). Realizable modification was chosen in the field of options of the turbulence models. The turbulence model  $k-\varepsilon$  makes it impossible to fully simulate the near-wall effects. Therefore the near-wall functions were used for the quality modeling of flows in ANSYS Fluent. Enhanced Wall treatment was chosen.

The natural gas was chosen from the data basis of ANSYS Fluent and given to the computed mesh. To solve the problems of gas dynamics we should consider gas compressibility. That is why the dependence of gas density on the flow parameters was set. For this purpose, the item Real-gas is chosen in the Density list, Materials menu. Besides, the equation of energy is automatically added to the equations being solved and gas temperature should be specified when boundary conditions are set. Steel is chosen as the material of the wall in the ANSYS Fluent database.

The Lagrangian discrete phase model is chosen in the menu Models to specify features of the discrete phase. The Set Injection Properties Window is opened in an Injection tab, where the surface of the particles supply (flow input), particles velocity and temperature at the inlet, the mass flow of particles, the maximum and minimum diameter of particle diameter range were chosen for each discrete phase (at first for the liquid and then for the solid one).

The velocity and temperature of discrete phase particles at the input of the shaped element was set as equal to the velocity and temperature of the continuous phase at the inlet. The velocity of the continuous phase at the shaped element inlet was determined by calculating the gas motion dynamics by shaped elements of compressor station manifold in ANSYS Fluent without accounting for the flow of the discrete phase [16]. The temperature of the continuous phase corresponds to the operating conditions of trunk gas pipelines. Moisture content of natural gases depends on the temperature and pressure of gas and it is determined by nomogram given in [17, Fig. 7]. The mass flow rate of the liquid phase was calculated based on the values of natural gas moisture and continuous phase volume flow.

According to [18] the mass flow of solids must not exceed  $0.001 \text{ g/m}^3$  in the natural gas. According to [19] the natural gas, which is fed into gas distribution points, contain much more impurities than  $0.001 \text{ g/m}^3$ . As the [20, Table 2] indicates, the weight of impurities can comprise to  $0.003 \text{ g/m}^3$  in the natural gas. The weight of impurities in the natural gas was assumed to be equal to  $0.003 \text{ g/m}^3$  at compressor station inlet before the purification system. The mass flow of the solid phase was calculated on the basis of the values of the mass of

solids in the natural gas and continuous phase volume flow.

When the natural gas passes through the purification system at the compressor station, the moisture and solid particles content is reduced. Accordingly, the mass flow of liquid and solid phases was reduced via shaped elements of a compressor station, located after the purification system in the flow direction.

The maximum diameter of the liquid phase droplets equals according to [20]

$$d_{cond}^{max} = \frac{2D_{in}}{(k_f We)^{\frac{2}{5}}} \left( \frac{\rho_{gas}}{\rho_{cond}} \right)^{\frac{2}{5}}, \quad (9)$$

where  $D_{in}$  is the internal diameter of the gas pipeline;  $k_f$  is the droplet drag coefficient,  $k_f = 0.4$ ;  $\rho_{gas}$  is the density of gas;  $\rho_{cond}$  is the density of the liquid phase;  $We$  is a dimensionless parameter – the Weber number

$$We = \frac{\rho_{gas} u^2 D_{in}}{\Sigma}, \quad (10)$$

where  $\Sigma$  is the surface tension force of the liquid phase on the brink of gas.

The strength of the surface tension of the liquid phase-gas interface depends on the pressure and temperature of gas and it is determined by [21].

The maximum diameter of the solid phase particles was taken as equal to the grain size of fine sand.

When natural gas passes through the purification system, diameter of liquid drops and solid phase particles reduces, that is why the maximum diameter of discrete phases was set smaller than it was calculated for the compressor station shaped elements, located after the purification system in the direction of the flow.

The Discrete Random Walk Model option was chosen in Turbulent Dispersion tab, Set injection properties window to account for the impact of the turbulent flow on the discrete phase.

The Erosion/Accretion option was marked in the Physical Models tab of the Lagrangian Discrete Phase model window to estimate the erosive wear.

In the Materials menu a corresponding material was chosen for each discrete phase of the ANSYS Fluent database. Because condensate, water and sand dominate in the natural gas, transported by pipelines, we have chosen the condensate of density  $\rho_{cond} = 960 \text{ kg/m}^3$  for the liquid phase, and the sand of density  $\rho_{sand} = 2800 \text{ kg/m}^3$  for solid particles.

Having set materials and characteristics of each discrete phase, the following boundary conditions were set in the Boundary Condition menu. Mass flow inlet was set at the inlet of the shaped element, and Pressure outlet was set at its outlet. When we set these boundary conditions of turbulence at the inlet of the shaped element, gas flow distribution is even in the cross section with the typical turbulent distribution diagram of gas flow rates. In addition to the values of the mass flow there were set the Turbulence Intensity 5%, Hydraulic

Diameter and gas temperature at the inlet in the Mass flow inlet window. When we set the pressure at the outlet, there were also set the Turbulence Intensity 5%, Hydraulic Diameter and the gas temperature at the outlet in the Pressure outlet window. Typically, the turbulence intensity does not exceed 20 %, but in most cases it is in the range of 1 to 10 %. The flow is considered completely turbulent when the turbulence intensity equals 5 %.

Wall boundary condition and the equivalent roughness coefficient of pipes  $h_s = 0.03 \text{ mm}$  were also set. In DPM Tab of the Wall boundary condition we have chosen the type of boundary condition for the Discrete Phase Reflection – reflection of the discrete phase particle from the wall (the angle of incidence equals to the angle of reflection).

Having set boundary conditions we tuned parameters of the solver. The Solution methods tab was chosen in the project tree, where the connection algorithm of gas motion and continuity equations were chosen in the Pressure-Velocity Coupling area. Then we chose Coupled algorithm, which was considered a separate type of the Coupled pressure-based solver. To connect the fields of velocity and pressure there was applied the splitting algorithm, and for other parameters – the setting algorithm. This algorithm makes it possible to get qualitative consistent results for virtually all classes of problems. To improve the stability of solution, the Courant number should be reduced to 50. Also, when parameters of the solver were set, the second order of accuracy was chosen for all equations.

The Navier-Stokes equations are solved by numerical method. Besides, differential equations are replaced by algebraic equations that describe the change in the variable between several neighboring points in an arbitrary mesh component. Analogous equations are solved by iterative method. After each iteration, some values of variables are calculated. They are substituted into the original equations, written in the following form  $f(p, T, \rho, x, y, z, v, w, \dots) = 0$ . Due to the fact that the solution is approximate (since the algebraic analogue is solved, not the differential equation), there is obtained that  $f(p, T, \rho, x, y, z, v, w, \dots) = R$  during the substitution of the calculation results. The value of  $R$  is called the discrepancy and it is the criterion for the process of solution. Obviously, the closer the value of  $R$  is to zero, the closer the solution of the discrete analog to the solution of the output differential equation.

The solution of the problem can be considered completed if the following conditions are met:

- the difference of the cost of a working body between input and output limits is close to zero and changes little from iteration to iteration;
- errors of all equations during calculation reach the values lower than the recommended limit;
- errors of all equations do not significantly change during the calculation.

The error of all equations, except energy equation, was set as  $R = 0.00001$ . The error for the energy equation was set as  $R = 1 \cdot 10^{-7}$ .

The simulation results were visualized in ANSYS Fluent Academic postprocessor, which helped to identify the places of the most intense liquid and solid particles hits of the walls of shaped elements and places for maximum erosive wear at shaped elements contours. For a better understanding of erosive wear of shaped elements of compressor station manifold one should read the study of the motion dynamics of multiphase flows through shaped elements of gas pipeline compressor station manifold [22] and studies of the gas motion dynamics by shaped elements of compressor station manifold [16].

Let us consider the compressor station manifold at its inlet where the welded T-junction with reinforcing patches is installed (Fig. 1), and where the gas is moving by the T-junction 1 run-pipe (Fig. 1) to the T-junction branch. The internal flush-jointed T-junction has an outside diameter of the run-pipe and the branch  $D_{out.r.p} = D_{out.b} = 1420$  mm, the nominal wall thickness of the run-pipe and the branch  $\delta_{r.p} = \delta_b = 28$  mm. The inner diameter of the run-pipe and the branch equal  $D_{in.r.p} = D_{in.b} = 1364$  mm. Geometry of the T-junction meets the requirements of the standard OST 102–61 [14]. The shaped element was drawn with the 3 meter surrounding areas of the pipeline and the outer diameter  $D_{out} = 1420$  mm. Pipe wall thickness was calculated, and then the pipes were chosen from the technical specifications, the nominal thickness of which equals  $\delta = 18.7$  mm. The inner diameter of the pipe is  $D_{in} = 1382.6$  mm and it is equal to the hydraulic diameter, which was set in ANSYS Fluent.

To study the erosive wear of the T-junction 1 compressor station manifold (Fig. 1), where the gas is moving by the T-junction run-pipe to the T-junction branch, there were set the following boundary conditions for the continuous phase in ANSYS Fluent preprocessor (Fig. 3, a)

1) inlet:

mass flow  $M_{in} = 697.9$  kg/s;

turbulence intensity 5 %;

hydraulic diameter  $D_{in} = 1.3826$  m;

gas temperature  $T_{in} = 297$  K;

2) outlet:

pressure  $P_{out} = 4930600$  Pa;

turbulence intensity 5 %;

hydraulic diameter  $D_{out} = 1.3826$  m;

gas temperature  $T_{out} = 297$  K.

There were set characteristics of every Discrete Phase at the inlet in Set injection properties Windows of the Discrete Phase Model (Fig. 3, a):

1) liquid phase (condensate):

velocity  $v_{cond} = 13.1$  m/s;

temperature  $T_{cond} = 297$  K;

mass flow  $M_{cond} = 0.58$  kg/s (according to nomogram given in [17, Fig. 7] moisture content of the natural gas is  $0.6$  g/m<sup>3</sup> when the pressure of the solid

phase equals 4.9 MPa and the temperature 297 K.

The mass flow of the liquid phase is calculated based on the volume flow rate of the continuous phase);

maximum diameter  $d_{cond}^{max} = 0.34$  mm;

minimum diameter  $d_{cond}^{min} = 3$  mm;

2) solid phase (sand):

velocity  $v_{sand} = 13.1$  m/s;

temperature  $T_{sand} = 297$  K;

mass flow  $M_{sand} = 2.1 \cdot 10^{-3}$  kg/s (mass of solids in the natural gas at a compressor station inlet before the purification system is assumed to be equal  $0.003$  g/m<sup>3</sup>).

The mass flow of the solid phase is calculated based on the volume flow rate of the continuous phase

maximum diameter  $d_{sand}^{max} = 0.12$  mm;

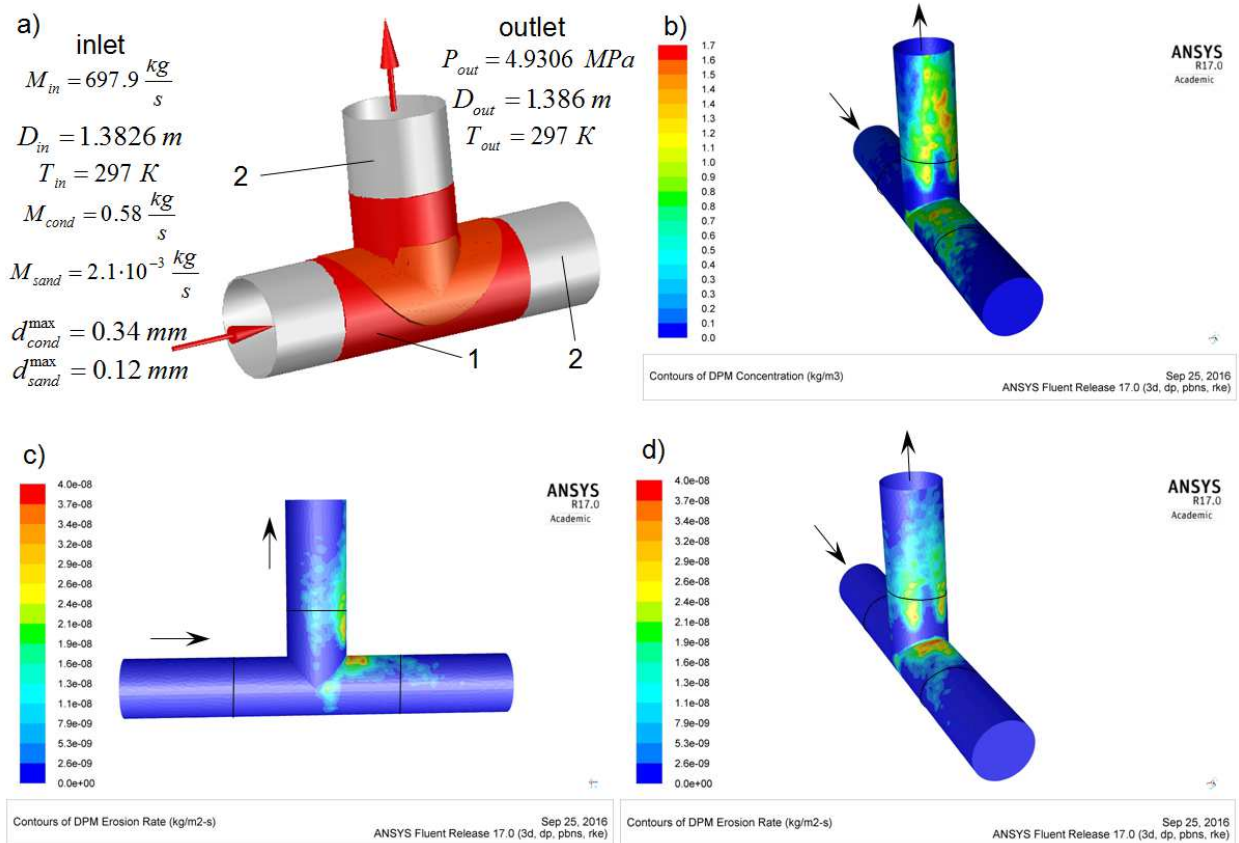
minimum diameter  $d_{sand}^{min} = 0.1$  mm.

When the gas flow passes through the internal flush-jointed T-junction with discrete phases, it changes its direction and flows from the T-junction run-pipe to the T-junction branch (Fig. 3). The simulation results were visualized in ANSYS Fluent Academic postprocessor by constructing concentration fields of the discrete phase (Fig. 3, b) and the fields of erosive wear rate (Fig. 3, c, d) on T-junction contours.

As can be seen from concentration fields of the discrete phase on T-junction contours (Fig. 3, b), liquid and solid particles hit most intensively the wall of the upper part of the T-junction run-pipe to the right of the branch and the walls of the T-junction branch and the adjacent pipe to the right (place of discrete phases hittings extends from the mid of the T-junction branch to more than 3 meters from the annular weld in the direction of the product's motion by the pipe adjacent to the branch). The maximum concentration of the discrete phase on contours of the T-junction run-pipe and branch equals 1.7 kg/s.

It is clear from the erosive wear fields on T-junction contours (Fig. 3, c, d) that the most intensive erosive wear of the T-junction is in the upper part of its run-pipe, to the right of the branch at the distance of 0.1 m from the T-junction branch. The maximum rate of erosive wear is equal to  $4.0 \cdot 10^{-8}$  kg/(m<sup>2</sup>·s). At this rate of erosive wear the wall becomes thinner at the speed of 0.158 mm/year. The erosive wear of less intensity is on the right of the branch and the run-pipe. The place of erosive wear extends from the mid of the branch at the distance of 1.5 m from the annular weld in the direction of the product's motion by the pipe adjacent to the branch. The maximum rate of erosive wear is equal  $2.5 \cdot 10^{-8}$  kg/(m<sup>2</sup>·s) at this point. The wall becomes thinner at the speed of 0.099 mm/year at this erosion rate.

Let us consider the compressor station manifold at its inlet where the bend with the rotation angle of 90° is installed (Fig. 1). An outside diameter of the pipe bend is  $D_{out.bend} = 1420$  mm, the nominal wall thickness of



1 – the internal flush-jointed T-junction with reinforcing patches 1420×28 – 1420×28 (OST 102–61 [10]);  
 2 – pipe 1420×18.7; a – design diagram; b – concentration fields of the discrete phase on contours;  
 c, d – erosive wear fields on contours

**Figure 3 – Simulation results of the erosive wear of the T-junction at the compressor station inlet, where the gas flows through the T-junction run-pipe to the T-junction branch**

the pipe bend is  $\delta_{bend} = 24 mm$ , and the inner diameter of the pipe bend equals  $D_{in,bend} = 1372 mm$ . Geometry of the bend meets the requirements of Gas Specifications 102-488/1 [11]. The shaped element was drawn with the surrounding areas of the pipeline 3 meters in length and the outer diameter  $D_{out} = 1420 mm$ . Pipe wall thickness was calculated, and then the pipes were chosen from the technical specifications, the nominal thickness of which equal  $\delta = 18.7 mm$ . The inner diameter of the pipe is  $D_{in} = 1382.6 mm$  and it is equal to the hydraulic diameter, which was set in ANSYS Fluent.

To study the erosive wear of the bend 2 of compressor station manifold (Fig. 1), there were set the following boundary conditions in ANSYS Fluent preprocessor:

- 1) inlet:  
 mass flow  $M_{in} = 697.9 kg/s$ ;  
 turbulence intensity 5 %;  
 hydraulic diameter  $D_{in} = 1.3826 m$ ;  
 gas temperature  $T_{in} = 297 K$ ;
- 2) outlet:  
 pressure  $P_{out} = 4.93 MPa$ ;  
 turbulence intensity 5 %;

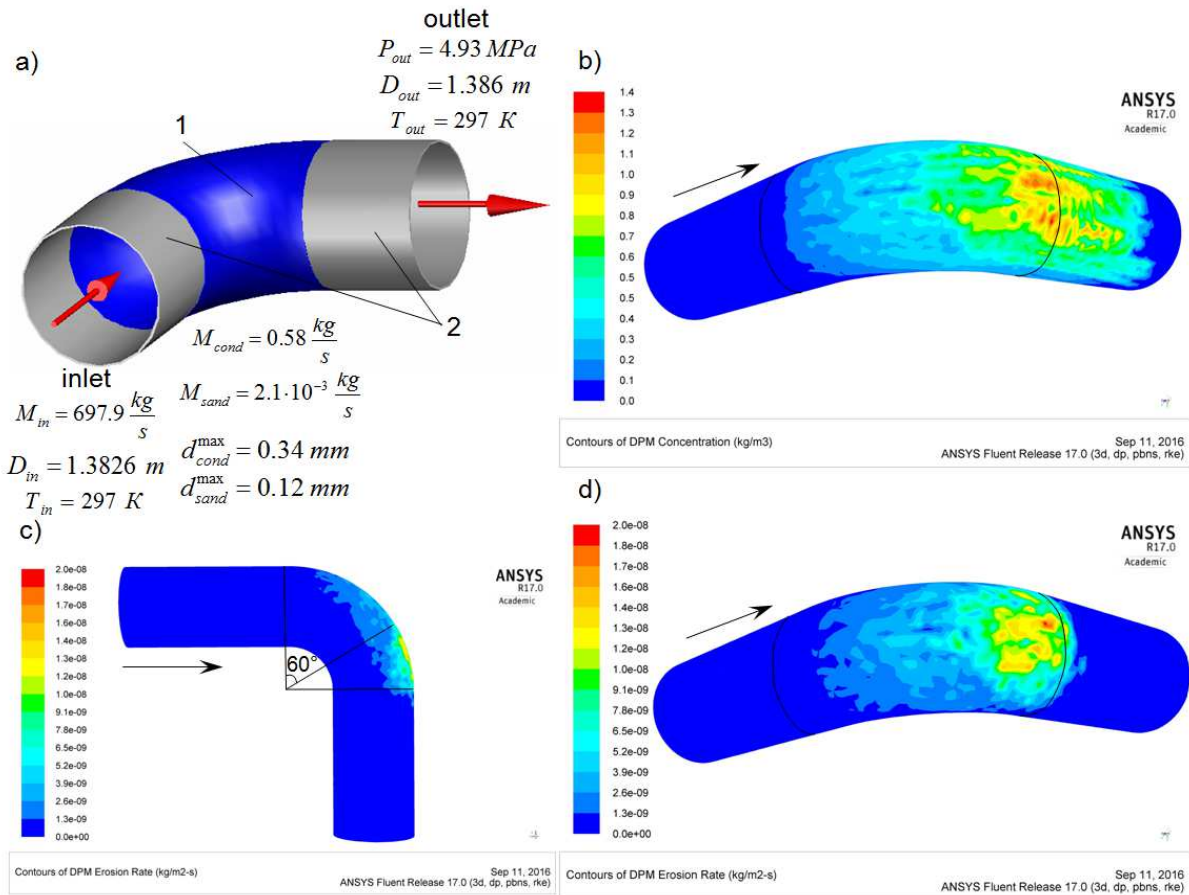
hydraulic diameter  $D_{out} = 1.3826 m$ ;  
 gas temperature  $T_{out} = 297 K$ .

Due to the fact that the bend 2 was placed near the internal flush-jointed T-junction 1 (Fig. 1), characteristics of every Discrete Phase at the bend inlet 2 (Fig. 4, a), which were set in Set injection properties Windows of the Discrete Phase Model, were the same as at the inlet of these T-junction.

The simulation results were visualized in ANSYS Fluent Academic postprocessor by constructing concentration fields of the discrete phase (Fig. 4, b) and the fields of erosive wear rate (Fig. 4, c, d) on the bend contours.

As can be seen from concentration fields of the discrete phase on bend contours (Fig. 4, b), liquid and solid particles hit most intensively the wall on its convex side. The place of hit extends from the mid of the bend to the distance of 1.5 m meters from the annular weld in the direction of the product's motion through the pipe adjacent to the bend. The most intensive hitting occurs on the convex side of the bend where the gas flows and at the beginning of the adjacent pipe (the maximum concentration of the discrete phase on contours equals 1.4 kg/s).

It is clear from the erosive wear fields on T-junction contours (Fig. 4, c, d) that the most intensive



1 – bend 90° 1420×24 (Gas Specifications 102–488/1 [11]); 2 – pipe 1420×18.7;  
 a – design diagram; b – concentration fields of the discrete phase on contours;  
 c, d – erosive wear fields on contours

**Figure 4 – Simulation results of the erosive wear of the bend at the compressor station inlet**

erosive wear is on the convex side of the bend where the gas stream flows between an angle of 60° and 90° of the bend and at the beginning of the pipe, which is welded to the bend, at the distance of 0.1 m in the direction of the product motion. The maximum rate of erosive wear is equal to  $2.0 \cdot 10^{-8} \text{ kg}/(\text{m}^2 \cdot \text{s})$ . At this rate of erosive wear the wall becomes thinner at the speed of 0.08 mm/year. The rate of erosive wear significantly decreases at the beginning of the pipe welded to the bend, although the intensive hittings of liquid and solid particles take place at the distance of 1.5 m from the annular weld. It is caused by the decrease of the angle of attack when the place of hitting moves away from the annular weld.

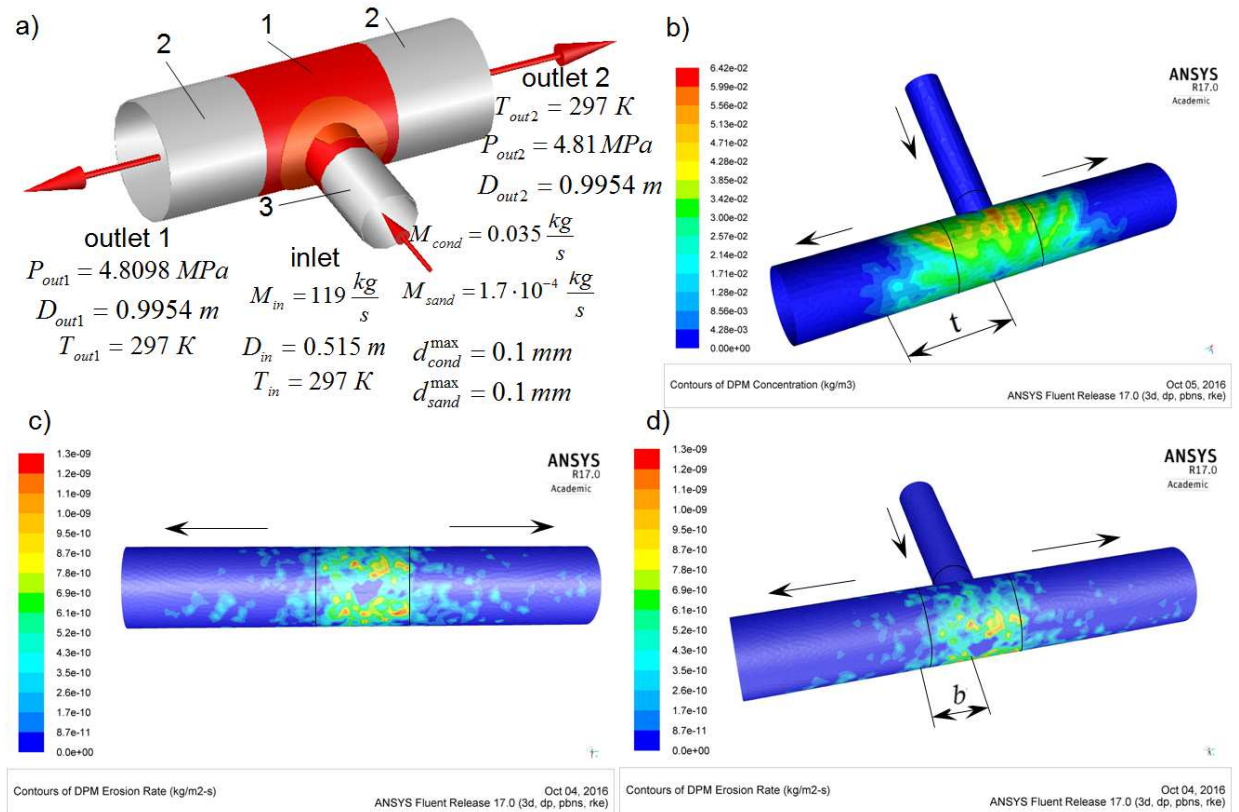
Let us consider the compressor station manifold at the outlet of the gas treatment unit where the welding T-junction 3 with reinforcing patches is installed (Fig. 1), and where gas moves by the T-junction branch and directs in two sides of the T-junction run-pipe (gas compressor unit GCU 1 and GCU 2). An outside diameter and the nominal wall thickness of the run-pipe and branch equal  $D_{out.r.p} = 1020 \text{ mm}$ ,  $D_{out.b} = 529 \text{ mm}$ ,  $\delta_{r.p} = 18 \text{ mm}$ ,  $\delta_b = 10 \text{ mm}$ , respectively. In this case the inner diameter of the run-pipe and branch equal

$D_{in.r.p} = 984 \text{ mm}$ ,  $D_{in.b} = 509 \text{ mm}$ , respectively.

Geometry of the T-junction meets the requirements of the standard OST 102–61 [14]. The shaped element was drawn with the surrounding areas of the pipeline. The length of the pipeline area, adjacent to the branch, is 1.7 m, and the outer diameter, the nominal wall thickness and the inner diameter are  $D_{out} = 529 \text{ mm}$ ,  $\delta = 7 \text{ mm}$ ,  $D_{in} = 515 \text{ mm}$ , respectively. The inner diameter of the pipeline areas adjacent to the T-junction is equal to the hydraulic diameter specified in ANSYS Fluent.

To study the erosive wear of the T-junction 3 of compressor station manifold (Fig. 1), where gas moves by the T-junction branch and directs in two sides of the T-junction run-pipe, there were set the following boundary conditions in ANSYS Fluent preprocessor:

- 1) inlet:  
 mass flow  $M_{in} = 119 \text{ kg/s}$ ;  
 turbulence intensity 5 %;  
 hydraulic diameter  $D_{in} = 0.515 \text{ m}$ ;  
 gas temperature  $T_{in} = 297 \text{ K}$ ;
- 2) outlet 1:  
 pressure  $P_{out1} = 4809800 \text{ Pa}$ ;  
 turbulence intensity 5 %;



1 – the internal flush-jointed T-junction with reinforcing patches 1020×18 – 529×10 (OST 102–61 [10]);  
 2 – pipe 1020×12.3; a – design diagram; b – concentration fields of the discrete phase on contours;  
 c, d – erosive wear fields on contours

**Figure 5 – Simulation results of the erosive wear of the compressor station manifold T-junction at the purification unit outlet, where the gas flows through the T-junction branch in two directions of the T-junction run-pipe**

hydraulic diameter  $D_{out1} = 0.9954 m$ ;  
 gas temperature  $T_{out1} = 297 K$ ;  
 3) outlet 2:  
 pressure  $P_{out2} = 4810000 Pa$ ;  
 turbulence intensity 5 %;  
 hydraulic diameter  $D_{out2} = 0.9954 m$ ;  
 gas temperature  $T_{out2} = 297 K$ .

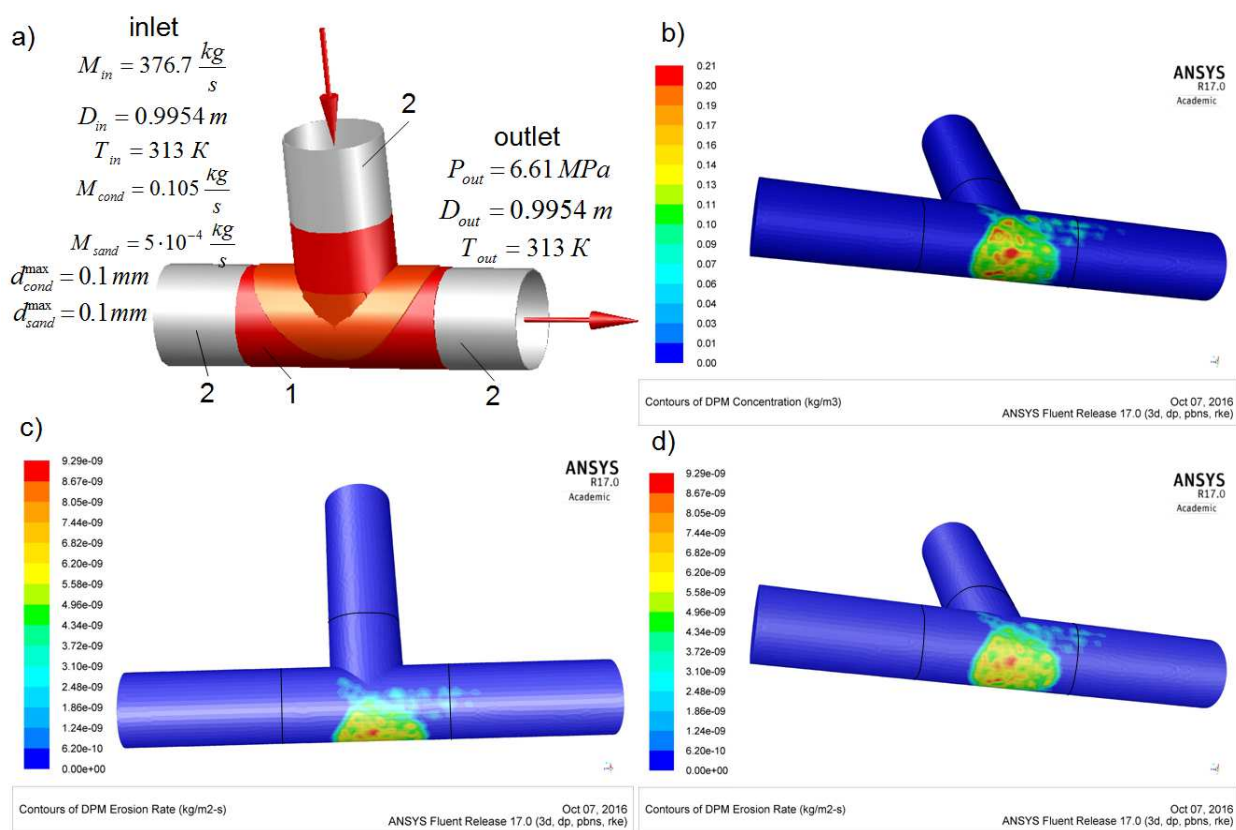
To determine the pressure at the outlet of the T-junction (Fig. 5, a) there was calculated the part of the flow (mass flow), which is directed toward the GCU 1, and which – toward GCU 2 (Fig. 1). Based on the values of the mass flow at the outlet of the T-junction run-pipe (Fig. 5, a) there were calculated the following values in ANSYS Fluent program complex: the T-junction for various pressures at the outlet 1 and outlet 2 of the T-junction run-pipe until there were determined the pressures, for which mass flows were equal to the pre-calculated at the T-junction run-pipe outlet. The pressures were equal to  $P_{out1} = 4809800 Pa$ ,  $P_{out2} = 4810000 Pa$ . Corresponding mass flows amounted  $M_{out1} = 70.4 kg/s$ ,  $M_{out2} = 48.6 kg/s$ .

There were set characteristics of every Discrete Phase at the inlet in Set injection properties Windows of the Discrete Phase Model (Fig. 5, a):

1) liquid phase (condensate):  
 velocity  $v_{cond} = 16.6 m/s$ ;  
 temperature  $T_{cond} = 297 K$ ;  
 mass flow  $M_{cond} = 0.035 kg/s$ ;  
 maximum diameter  $d_{cond}^{max} = 0.1 mm$ ;  
 minimum diameter  $d_{cond}^{min} = 0.1 mm$ ;  
 2) solid phase (sand):  
 velocity  $v_{sand} = 16.6 m/s$ ;  
 temperature  $T_{sand} = 297 K$ ;  
 mass flow  $M_{sand} = 1.7 \cdot 10^{-4} kg/s$ ;  
 maximum diameter  $d_{sand}^{max} = 0.1 mm$ ;  
 minimum diameter  $d_{sand}^{min} = 0.1 mm$ .

During the movement of gas with discrete phases by the T-junction 1 (Fig. 5), there occurs bifurcation of gas flow and it is directed in two opposite directions of the T-junction run-pipe. The calculation results are visualized in ANSYS Fluent post-processor by constructing concentration fields of the discrete phase (Fig. 5, b) and the fields of erosion rate (Fig. 5, c, d) on the T-junction contours.

As can be seen from concentration fields of the discrete phase on the T-junction contours (Fig. 5, b), the place of the most intensive hitting of liquid and solid



1 – the internal flush-jointed T-junction with reinforcing patches 1020×20 – 1020×20 (OST 102–61 [10]);  
 2 – pipe 1020×12.3; a – design diagram; b – concentration fields of the discrete phase on contours;  
 c, d – erosive wear fields on contours

**Figure 6 – Simulation results of the T-junction erosive wear at the outlet of the gas treatment unit 1, where the gas flows through the T-junction branch in one direction of the T-junction run-pipe**

particles has the form of a ring with a width of  $t = 1.5 m$ , curved by the inner surface of the T-junction run-pipe and adjacent pipes. The maximum concentration of a discrete phase is insignificant on the T-junction run-pipe contours, because the discrete phase is dispersed upon a large internal surface area and is  $0.064 kg/s$  in the T-junction run-pipe.

As can be seen from concentration fields on the T-junction contours (Fig. 5, c, d), the place of the most intensive T-junction erosive wear is in the T-junction run-pipe, opposite to the branch and also has an annular form with a width of  $b = 1.5 m$ , curved by the inner surface of the T-junction run-pipe. The maximum erosive wear is insignificant and equals  $1.3 \cdot 10^{-9} kg/(m^2 \cdot s)$ . At this rate of erosive wear the wall becomes thinner at the speed of  $0.0052 mm/year$ .

Let us consider the compressor station manifold at the outlet of the gas treatment unit 1 where the welding T-junction 4 with reinforcing patches is installed (Fig. 1), and where gas moves through the T-junction branch and directs in one side of the T-junction run-pipe. An outside diameter of the run-pipe and branch is  $D_{out.r.p} = D_{out.b} = 1020 mm$ , and the nominal wall thickness of the run-pipe and branch equal  $\delta_{r.p} = \delta_b = 20 mm$ . The inner diameter of the run-pipe

and the branch equals  $D_{in.r.p} = D_{in.b} = 980 mm$ . Geometry of the T-junction meets the requirements of the standard OST 102–61 [14]. The shaped element was drawn with the surrounding areas of the 3-meter pipeline and the outer diameter  $D_{out} = 1020 mm$ . The pipe wall thickness was calculated, and then the pipes were chosen from the technical specifications, the nominal thickness of which equals  $\delta = 12.3 mm$ . The inner diameter of the pipes is  $D_{in} = 995.4 mm$  and it is equal to the hydraulic diameter, which was set in ANSYS Fluent.

To study the gas motion dynamics through the T-junction 4 of the compressor station manifold (Fig. 1), where the gas moves through the T-junction branch to one direction of the T-junction run-pipe, there were set the following boundary conditions in ANSYS Fluent preprocessor (Fig. 6, a):

- 1) inlet:  
 mass flow  $M_{in} = 376.7 kg/s$ ;  
 turbulence intensity 5 %;  
 hydraulic diameter  $D_{in} = 0.9954 m$ ;  
 gas temperature  $T_{in} = 313 K$ ;
- 2) outlet:  
 pressure  $P_{out} = 6.61 MPa$ ;  
 turbulence intensity 5 %;

hydraulic diameter  $D_{out} = 0.9954$  m;

gas temperature  $T_{out} = 313$  K.

The Discrete Phase Model was set with characteristics of every Discrete Phase at the inlet in Set injection properties Windows (Fig. 6, a):

1) liquid phase (condensate):

velocity  $v_{cond} = 10$  m/s;

temperature  $T_{cond} = 297$  K;

mass flow  $M_{cond} = 0.105$  kg/s;

maximum diameter  $d_{cond}^{max} = 0.1$  mm;

minimum diameter  $d_{cond}^{min} = 1$  mm;

2) solid phase (sand):

velocity  $v_{sand} = 10$  m/s;

temperature  $T_{sand} = 297$  K;

mass flow  $M_{sand} = 5 \cdot 10^{-4}$  kg/s;

maximum diameter  $d_{sand}^{max} = 0.1$  mm;

minimum diameter  $d_{sand}^{min} = 0.1$  mm.

When the gas flow with a Discrete Phase runs through the T-junction 4 of the compressor station manifold, placed at the outlet of the gas treatment unit 1 (Fig. 1), it changes its direction and runs from the branch to the right side of the T-junction run-pipe (Fig. 6).

The simulation results were visualized in ANSYS Fluent Academic postprocessor by constructing concentration fields of the discrete phase (Fig. 6, b) and the fields of erosive wear rate (Fig. 6, c, d) on the T-junction contours.

As can be seen from concentration fields of the discrete phase on T-junction contours (Fig. 6, b), liquid and solid particles hit most intensively the wall of the T-junction run-pipe opposite to the branch. The place of hit is pear shaped. The annular part of the pear shaped place of hit almost coincides with the projection of the T-junction branch on the inner wall of the run-pipe. An elongated part of the pear-shaped place of hit extends in the direction of the product's motion through the T-junction line, approximating to internal flush-jointed pipe at the distance of 0.3 m. The maximum concentration of a discrete phase on the T-junction contours is 0.21 kg/s.

It is clear from the erosive wear fields on T-junction contours (Fig. 6, c, d) that the place of the most intensive erosive wear of the T-junction coincides with the place of the most intensive hit of liquid and solid particles to the wall and is pear shaped and of the same size. The maximum rate of erosive wear is equal to  $1.3 \cdot 10^{-9}$  kg/(m<sup>2</sup> · s). At this rate of erosive wear the wall becomes thinner at the speed of 0.0052 mm/year.

## Conclusions

Based on the Lagrangian approach there was studied for the first time the erosive wear of shaped elements of compressor station manifold of the gas pipeline, the design and geometric dimensions of which are identical to production prototypes, using ANSYS Fluent Academic software. There are identified the

places of intensive hits of condensate droplets and solid particles, carried by the gas flow, to the pipeline wall, places of the maximum erosive wear of bends, T-junctions of compressor station manifold and adjacent pipeline sections, and there is calculated the erosion rate.

It was found out that the most intensive erosive wear of the bends is on their convex side where the gas stream flows between an angle of 60° and 90° of the bend and at the beginning of the pipe, which is welded to the bend. The place of erosive wear depends on the scheme of the gas motion through the T-junction. If gas flows through the T-junction run-pipe to the T-junction branch, the most intensive erosive wear is in the upper part of the run-pipe in the side of the branch opposite to the inlet cross section, and it is opposite to the inlet cross section side in the branch and adjacent pipe. If gas flows through the T-junction branch to the two sides of the T-junction run-pipe, the most intensive erosive wear is in the T-junction run-pipe in the opposite to the inlet cross section side of the branch and it is of the annular form curved by the inner surface of the T-junction run-pipe. If gas flows through the T-junction branch in one direction of the T-junction run-pipe, the most intensive erosive wear of the T-junction is pear shaped and placed opposite to the T-junction branch.

These studies open the prospect for a full and comprehensive investigation on the shaped elements strength of compressor station manifold.

## References

- [1] Abdolkarimi, V & Mohammadikhah, R 2013, 'CFD modeling of particulates erosive effect on a commercial scale pipeline bend', *ISRN Chemical Engineering*, vol. 2013, pp. 1–10.
- [2] Abdua, A 2011, *Estimating erosion in oil and gas pipe line due to sand presence*, Karlskrona, Sweden.
- [3] Azimian, M & Bart, H 2014, 'Investigation of hydroabrasion in slurry pipeline elbows and T-junctions', *Journal of Energy and Power Engineering*, no. 8, pp. 8–65.
- [4] Mazumder, Q 2012, 'Effect of Liquid and Gas Velocities on Magnitude and Location of Maximum Erosion in U-Bend', *Journal of Fluid Dynamics*, no. 2, pp. 29–34.
- [5] Zhang, H, Tan, Y & Yang, D 2012, 'Numerical investigation of the location of maximum erosive wear damage in elbow: Effect of slurry velocity, bend orientation and angle of elbow', *Powder Technology*, no. 217, pp. 467–476.
- [6] Hongjun, Z, Yuanhua, L & Guang, F 2013, 'Numerical analysis of flow erosion on sand discharge pipe in nitrogen drilling', *Advances in Mechanical Engineering*, vol. 2013, pp. 1–10.
- [7] Dorina, I 2012, 'Reduction of pipe wall erosion by creating a vortex flow in anthracite powder pneumatic transport for power plants', *International conference on renewable energies and power quality (ICREPQ'12)*, Santiago de Compostela: European Association for the Development of Renewable Energies, Environment and Power Quality (EA4EPQ). [30 March 2012].
- [8] Hadžiahmetović, H, Hodžić, N, Kahrmanović, D & Džaferović, E 2014, 'Computational fluid dynamics (CFD) based erosion prediction model in elbows', *Technical Gazette* 21, no. 2, pp. 275–282.

- [9] Tarek, M, Walid, A, Soubhi, H & Hamdy, O 2011, 'CFD Simulation of Dilute Gas-Solid Flow in 90° Square Bend', *Energy and Power Engineering*, no. 3, pp. 246–252.
- [10] Industry Standard 1981, *Steel welded details of the main pipelines of up to 10.0 MPa (100 kgf/cm<sup>2</sup>). Welded T-junctions with reinforcing patches. Dimensions*, OST 102-61-81, Ministry of Construction of Oil and Gas Industry Enterprises.
- [11] Specifications 2005, *Connecting parts for main gas pipelines up to 9.8 MPa (100 kgf/cm<sup>2</sup>)*, Gas Specifications 102-488/1-05, JSC Trubodetal.
- [12] Squires, K & Eaton, J 1990, 'Particle response and turbulence modification in isotropic turbulence', *Phys. Fluid*, vol. 2, no. 7, pp. 1191–1203.
- [13] Hinze, JO 1975, *Turbulence*, McGraw-Hill, New York.
- [14] Kochevskyi, AN 2004, Possibilities of fluid and gas flows modeling using modern software products, *Herald of Sumy State University, Technical Sciences*, no.3, pp. 5–20.
- [15] Finnie, I & Kabil, Y 1965, 'On the formation of surface ripples during erosion', *Wear*, no. 8, pp. 60–69.
- [16] Doroshenko, YaV, Marko, TI, Doroshenko, YuI 2016, 'Study of the gas movement dynamics by the shaped elements of compressor station manifold', *Scientific Herald*, no.1 (40), pp. 60–69.
- [17] Kotliar, IYa, Piliak, VM 1971, 'Operation of gas pipelines', Nedra, Leningrad. (in Russian).
- [18] State Standard 1994, *Combustible natural gases for industrial and municipal purposes. Specifications*, State OST 5542-87, Publishing House of Standards.
- [19] Usachev, AP, Shurait, AL, Zhelanolov, VP, Nedlin, MS, Demchuk, VYu, Zubailov GI 2009, 'Analysis of dangerous joint effects of mechanical particles and disproportionate efforts on the elements of gas control points', *Scientific and technical problems of improving and developing gas supply systems, A collection of scientific papers*, pp. 4–14.
- [20] Sinaisky, EG, Lapiga, EYa, Zaitsev, YuV 2002, *Separation of multiphase multicomponent systems*, LLC Nedra-Business Center, Moscow. (in Russian).
- [21] Gimatudinov, ShK 1971, *Physics of the Oil and Gas Reservoir*, Nedra, Moscow. (in Russian).
- [22] Doroshenko, YaV, Marko, TI, Doroshenko, YuI 2016 'Study of the multiphase flows movement dynamics by the shaped elements of compressor station manifold', *International Scientific Journal*, no.7, pp. 68–77.

УДК 622.691.4

## Дослідження ерозійного зношування фасонних елементів обв'язки компресорної станції магістрального газопроводу

Я. В. Дорошенко, Т. І. Марко, Ю. І. Дорошенко

Івано-Франківський національний технічний університет нафти і газу;  
вул. Карпатська, 15, м. Івано-Франківськ, 76019, Україна

Дослідження виконані з метою виявлення місць інтенсивного ударяння рідких і твердих частинок до стінки фасонних елементів обв'язки компресорної станції магістрального газопроводу, місць їх ерозійного зношування та розрахунку величини ерозійного зношування.

Здійснено 3D-моделювання обв'язки компресорної станції і її фасонних елементів, де відбувається складний рух багатофазних потоків, зміна напрямку їх руху, завихрення, ударяння дискретних фаз до стінки трубопроводу, ерозійне зношування стінки труби.

На основі лагранжевого підходу (модель Discrete Phase Model) розроблено методику моделювання ерозійного зношування фасонних елементів обв'язки компресорної станції (відводів, трійників) із застосуванням програмного комплексу ANSYS Fluent R17.0 Academic. Математична модель базується на розв'язанні системи рівнянь Нав'є–Стокса, нерозривності, руху дискретних фаз, рівняння Фінні, замкнених двопараметричною  $k-\varepsilon$  моделлю турбулентності Лаундера–Шарма з відповідними початковими та граничними умовами. У трійниках моделювання виконувалось для різних схем руху газу (газ рухається магістраллю трійника і з магістралі направляється у відвід трійника; газ рухається відводом трійника і з нього спрямовується у магістраль трійника, в якій частина газового потоку перетікає в одну з сторін магістралі, а друга – в іншу; газ рухається відводом трійника і з нього спрямовується в одну із сторін магістралі трійника).

Результати моделювання були візуалізовані в постпроцесорі ANSYS Fluent R17.0 Academic побудовою полів концентрацій дискретної фази та полів швидкостей ерозійного зношування на контурах фасонних елементів. За результатами досліджень виявлено місця інтенсивного ударяння рідких і твердих частинок до стінки фасонних елементів обв'язки компресорної станції, місця інтенсивного ерозійного зношування стінки трубопроводу, розраховано величину ерозійного зношування.

Ключові слова: відвід, дискретна фаза, підхід Лагранжа, поля концентрації, рівняння Фінні, трійник.